cluster deposition. As the CO ligands are lost, the cluster collapses and condenses to a solid material similar to that produced in the sputtering experiments at the same N/H ratio. This is perhaps reasonable as exo-cluster ligand bonding is known to constitute the largest fraction of the disruption energy of metal carbonyl clusters.[27] In addition, once one strips the ligands off from a cluster, the residual bonding of the remaining core is far from that of the stable solid. Hence, the question of whether or not a given cluster stoichiometry will serve to determine the material stoichiometry depends not only on the properties of the cluster itself but also on those of the material. In the case of borides where Fe_xB clusters are thought to be elements of the amorphous structure, discrete cluster precursor stoichiometry does appear to define the B:Fe ratio.[26]

In conclusion, we have demonstrated that a discrete nitrido cluster can be used in the preparation of thin iron nitride films by chemical vapor deposition at relatively low temperatures. The films have properties very similar to those formed by reactive sputtering in $Ar/N_2/H_2$ systems with the same N/H ratio as the discrete nitrido cluster.

Acknowledgment. The support of the Army Research Office (Contract DAAL03-86-K-0136, M.M.A., T.P.F.) and the donors of the The Petroleum Research Fund, administered by the American Chemical Society (G.J.L.), is gratefully acknowledged. T.P.F. thanks Prof. M. Lagally, A. Lefkow, and Dr. Ngoc C. Tran of the Thin Film Institute of the Univeristy of Wisconsin for their assistance in carrying out part of this work and their hospitality during the tenure of a Guggenheim Fellowship.

(27) Connor, J. A. *Top. Curr. Chem.* **1977**, *71*, 71.

In Situ Photodegradation of $SnBr_2$

R. Ken Force,† Mebrahtu G. Fessehaie,‡ Robert P. Grosso,‡ John M. Laliberte,‡ Skye McClain,‡ William S. Willis,‡ and Steven L. Suib*,‡,§

Department of Chemistry, University of Rhode Island, Kingston, Rhode Island 02881; Department of Chemistry and Institute of Materials Science, University of Connecticut, Storrs, Connecticut 06268; and Department of Chemical Engineering, University of Connecticut, Storrs, Connecticut 06268

Received October 4, 1989

The in situ photodegradation of $SnBr_2$ has been studied under vacuum or under nitrogen with X-ray photoelectron spectroscopy, residual gas analysis, photogravimetric analysis, and thermogravimetric analysis. Our results suggest that the photodegradation process is quite complex and occurs through several pathways. The initial step involves the photoexcitation of $SnBr_2$ with evolved gaseous species containing SnBr(g) and Br(g) as major decomposition products. In addition, water molecules on the $SnBr_2$ form SnO(s) and HBr. Minor secondary pathways for the decomposition involve the dissociation of HBr and SnBr(g). In addition, some metallic Sn is formed during photolysis.

Introduction

Some semiconducting metal oxides have been shown to be reduced with light to the metallic state if the bandgap of the semiconducting metal oxide is greater in energy than the reverse of the heat of formation of the metal oxide.[1-5] All of this type of research studied to date has concerned photoreduction of metal oxides in the powdered state. For example, Fleisch and Mains[1-5] used X-ray photoelectron spectroscopy to study the photoreduction of CuO, PdO, PtO, WO_3, MoO_3, and ZnO. They found that metallic Cu, Pd, and Pt could be formed via photolysis but that only partial reduction of the molybdenum and tungsten oxide systems occurred. ZnO was not photoreduced, and Fleisch and Mains suggested that this was because the bandgap of the ZnO was less energetic than the reverse of the heat of formation of ZnO.

This theory concerning bandgaps and thermodynamic parameters has not been tested with semiconducting materials other than oxides. In addition, there are a number of interesting questions regarding this theory that could be tested experimentally. Some of the questions that were apparent to use are the following: (1) Can this theory be applied to semiconductors besides metal oxides? (2) Can fragments of metal oxide be deposited on various surfaces and photoreduced? (3) Are other factors such as the nature of surface functional groups important in this photoreduction process?

This paper concerns the photolysis of a semiconducting metal halide complex, $SnBr_2$. The band gap[6] of $SnBr_2$ is 328.3 kJ/mol, and the heat of formation is −243.3 kJ/mol. According to the theory postulated by Fleisch and Mains,[5] $SnBr_2$ should be photoreduced to metallic Sn. We have investigated the photolytic behavior of $SnBr_2$ using several different spectroscopic and gravimetric methods. To monitor changes in the oxidation state of the $SnBr_2$, in situ photolytic X-ray photoelectron spectroscopy measure-

† University of Rhode Island.
‡ Department of Chemistry and Institute of Materials Science, University of Connecticut.
§ Department of Chemical Engineering, University of Connecticut.
* Author to whom correspondence should be addressed.

(1) Fleisch, T. H.; Mains, G. J. *J. Phys. Chem.* **1986**, *90*, 5317-5320.
(2) Fleisch, T. H.; Mains, G. J. *J. Chem. Phys.* **1982**, *76*, 780-786.
(3) Fleisch, T. H.; Zajak, G. W.; Schreiner, J. O.; Mains, G. J. *Appl. Surf. Sci.* **1986**, *26*, 488-497.
(4) Fleisch, T. H.; Mains, G. J. *Appl. Surf. Sci.* **1982**, *10*, 50.
(5) Mains, G. J.; Schreiner, J. O.; Flesich, T. H. *J. Phys. Chem.* **1981**, *85*, 4084-4089.
(6) Strehlow, W. H.; Cook, E. L. *J. Phys. Chem. Ref. Data* **1973**, *2*, 163-193.

0897-4756/90/2802-0268$02.50/0

Table I. Binding Energies of Tin(II) Bromide Samples[a]

sample	conditions	Sn M5	Sn M4	Sn3	Sn5	C	Br	O
C	initial	829.1	822.3	495.8	487.3	a	68.9	532.2
	+60 min, *hν*	827.9	820.6	495.1	486.6	a	68.9	530.4
C	initial	828.7	822.1	495.5	487.1	a	69.0	532.3
		830.3	*820.7*	*531.2*				
	+60 min 180 °C	828.7	821.6	495.4	487.0	a	68.9	531.8
	+60 min, *hν*	827.8	820.6	495.0	486.6	a	68.5	530.3
								532.2
S	initial	828.6	821.1	495.3	487.0	a	68.6	530.8
								527.0
	+60 min, *hν*	828.2	820.7	495.1	486.7	a	68.4	532.1
								530.7
C, HP	initial	828.6	821.2	495.3	486.9	a	69.0	532.1
								530.9
	+60 min, *hν*	828.0	820.6	495.1	486.7	a	68.5	530.5
S	initial	828.5	821.2	495.5	487.0	a	68.9	526.3
						280.4		530.9
	+60 min, 180 °C	828.5	821.3	495.4	487.1	a	69.0	526.4
						280.4		530.9
	+60 min, *hν*	827.7	821.3	495.1	486.7	a	68.5	527.0
				491.4		280.8	65.3	530.6

[a] Italicized values indicate weak peaks and shoulders. C, commercial $SnBr_2$; S, synthesized $SnBr_2$. Transitions are Sn $Me_5N_{45}N_{45}$, Sn $M_4N_{45}N_{45}$, Sn $3d_{3/2}$, Sn $3d_{5/2}$, C 1s, Br 3d, O 1s. + means in addition to the above treatment. HP signifies pelletized at ultrahigh pressure. All samples have Mo holders.

ments were done. During photolysis, residual gas analyses were carried out to determine the nature of the gas-phase volatile species being emitted from $SnBr_2$. Thermogravimetric analyses[7] were done to study the thermal stability of $SnBr_2$ and to test whether the effects that we suggest are due to photolysis are solely photochemical effects. Finally, we have conducted some photogravimetric analyses on $SnBr_2$ to show that there is a significant weight loss of the starting $SnBr_2$ material during photolysis. The increase in temperature of $SnBr_2$ during photolysis was measured, and separate thermal activation of $SnBr_2$ to these temperatures did not lead to the same products observed during photolysis. A series of chemical reactions have been outlined for the photodecomposition process and will be presented.

Experimental Section

Surface Science Experiments. Sample Mounting Procedures. Samples of $SnBr_2$ were pelletized in a pellet press to pressures between 10 000 and 50 000 psi. After being pelletized, samples were mounted on a Mo metal substrate in order to cover the sample rod holder during analyses. A Mo holder was used in all surface experiments to provide good electrical contact to the spectrometer as well. Transitions for Mo were not observed in these experiments, indicating that the $SnBr_2$ samples entirely covered the Mo.

X-ray Photoelectron Spectroscopy Methods. X-ray photoelectron spectroscopy (XPS) experiments were done with a Leybold Heraeus LHS-10 spectrometer with an EA-10 hemispherical energy analyzer and either Mg Kα or Al Kα X-rays.[8] X-ray beam voltages of 13 kV and beam currents of 10 mA were used. A gold $4f_{7/2}$ binding energy of 83.8 eV and a Cu $2p_{3/2}$ binding energy of 932.4 eV were used for calibration of the binding energy scale. In general, a survey (wide) scan was collected prior to narrow scans of specific elements. Survey scans were collected in the constant relative resolution mode with a retarding factor of 3. A constant absolute resolution mode was used for narrow scans. The C 1s transition was used to calibrate the binding energy scale, and the C 1s peak was set to 284.6 eV. All semiquantitative analyses and binding energy positions were determined from narrow scans. Specific transitions reported in this work include the Sn M_5N_{45}, Sn $M_4N_{45}N_{45}$, O 1s, Sn $3d_{3/2}$, Sn $3d_{5/2}$, C 1s, and Br 3d.

Photolysis Experiments. A Xe lamp having emission in the 250–800-nm range was used for all photolysis experiments. The in situ photolyses were done in a preparatory chamber of the surface spectrometer by irradiating the solid powder through a JENA glass window with the 100-W Xe lamp manufactured by Oriel Corp. During photolyses the pressure in this preparatory chamber did not exceed 1×10^{-6} mbar. The light was focused into the spectrometer by a 100-mm focal length concave mirror. Samples of $SnBr_2$ were analyzed with XPS methods before and after irradiation.

Residual Gas Analysis. An Inficon Model IQ 200 residual gas analyzer (RGA) was used to analyze volatile gases evolved during the photolyses.[9] The mass range of the RGA was calibrated with a mixture of inert gases including He, Ne, Xe, and Ar. Branching ratios of different species found in the literature[10] were used to identify the residual gases.

Photogravimetric Analyses. Photogravimetric analysis (PGA) experiments were done on a Du Pont 9900 thermogravimetric analyzer by irradiating $SnBr_2$ with a 450-W Xe lamp made by Electronics Measurement, Inc. Samples were loaded into quartz or Pyrex holders, and a thermocouple was used to measure the temperature of the sample during irradiation. No external temperature ramp was applied during these experiments. Sample size ranged from 50 to 140 mg. During these experiments the light was turned on and off in order to determine the direct effect of the irradiation. Experiments were carried out for as long as 150 min.

Thermogravimetric Analyses. Thermogravimetric analyses[7] (TGA) were done on the same instrument described above under photogravimetric analyses; however, an external temperature ramp was applied to the sample with no concomitant irradiation.

Synthesis of $SnBr_2$. Commercial grade $SnBr_2$ (Alfa Ventron) was used for some experiments. The major contaminant of this material was chloride ion. Synthesis of pure $SnBr_2$ was done by adding HBr to Sn powder according to literature procedures.[11] To minimize contamination of the sample, the experiment was carried out in the dark under nitrogen gas. A Mohr titration was done to determine the relative amounts of chloride ion in the commercial and the synthesized $SnBr_2$ samples.[12]

(7) Carrado, K. A.; Kostapapas, A.; Suib, S. L. *Solid State Ionics* **1988**, *6*, 77–86.
(8) Winiecki, A. M.; Suib, S. L. *Langmuir* **1989**, *5*, 333–338.
(9) Morse, B. M.; Suib, S. L. *Langmuir* **1989**, *5*, 1340–1343.
(10) (a) Berkowitz, J.; Marquardt, J. R. *J. Chem. Phys.* **1963**, *39*, 275–283. (b) Colin, R.; Drowart, J. Univ. Libre, Brussels, Belgium, AD, 607,792, 1966. (c) Lyubimov, A. P.; Bespaltseva, I. I. *Izv. Nauk SSSR* **1969**, *5*, 1289–1290. (d) Hiroyama, C.; Straw, R. D. *Thermochim. Acta* **1984**, *80*, 297–305. (e) Buchanan, A. S.; Knowles, D. J.; Swingler, D. L. *J. Phys. Chem.* **1969**, *73*, 4394–4397.
(11) Brauer, G. *Handbook of Preparative Inorganic Chemistry*, Academic Press: New York, 1963; Vol. 1, pp 732–733.
(12) Fischer, R. B.; Peters, D. G. *Quantitative Chemical Analysis*; W. B. Saunders: Philadelphia, 1969; pp 253–254.

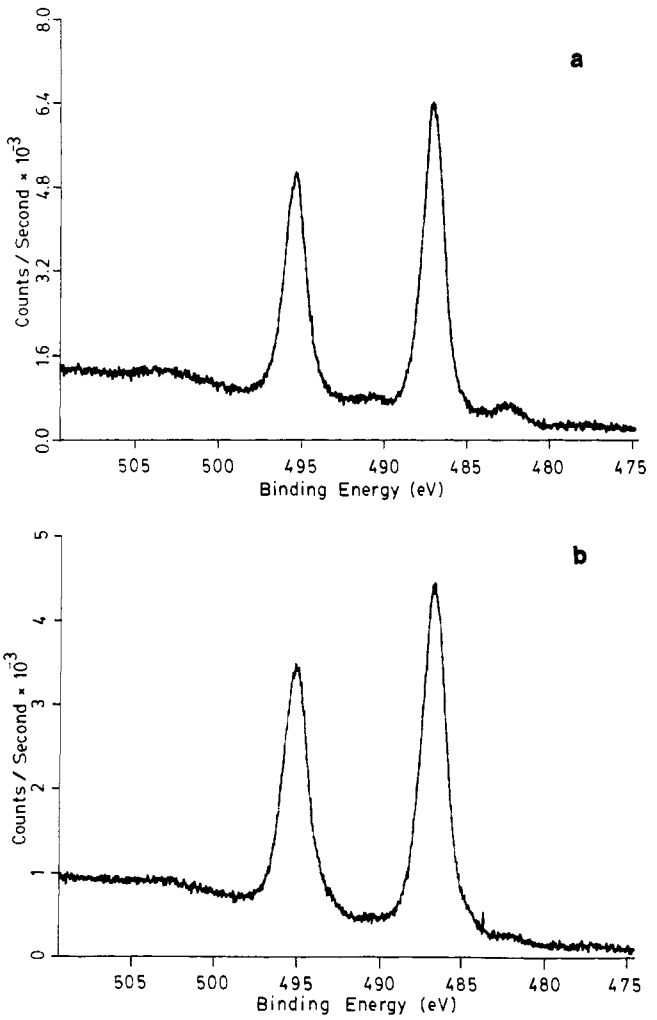

Figure 1. X-ray photoelectron Sn $3d_{3/2}$ spectra for impure $SnBr_2$ on Mo: (a) no irradiation; (b) irradiated with 1000-W Xe lamp for 40 min.

Differential Scanning Calorimetry. Differential scanning calorimetry experiments were done on a Du Pont 9900 DSC apparatus. Samples were loaded into aluminum sample pans.

Results

X-ray Photoelectron Spectroscopy. The binding energies for the Sn $M_5N_{45}N_{45}$, Sn $M_4N_{45}N_{45}$, O 1s, Sn $3d_{3/2}$, $Sn3d_{5/2}$, C 1s, and Br 3d transitions for a variety of samples are given in Table I. There are two types of $SnBr_2$ studied here, which we refer to as commercial and synthetic $SnBr_2$. The commercial $SnBr_2$ was obtained from Alfa Ventron Co. and was found to contain high levels (>10 ppm) of organic acetate and chloride ion contaminants. The synthetic $SnBr_2$ was prepared according to literature procedures.[11] The commercial and synthetic $SnBr_2$ pellets were mounted on Mo and treated under various conditions as shown in Table I. XPS data for the seven transitions listed above are given for the samples prior to irradiation and after irradiation. In certain cases, the samples were heated prior to irradiation to allow the evolution of water and other volatile surface species.

The data of Table I show that more than one peak appears primarily in the O 1s region either before or after photolysis. The binding energies of these transitions do not significantly change after photolysis.

Thermal treatment of the $SnBr_2$ samples prior to photolysis does not have a marked effect on the binding energies of the Sn, O, C, or Br transitions. Pressing a pellet of $SnBr_2$ at high pressure (50 000 psi) also does not seem to affect the binding energies in a significant way.

Table II. Relative Elemental Ratios for Tin(II) Bromide Samples[a]

sample	conditions	O	C	Br
C	initial	139	213	195
	+60 min, $h\nu$	133	215	117
C	initial	166	409	186
	+60 min, 180 °C	144	413	174
	+60 min, $h\nu$	91	220	131
S	initial	212	334	160
	+60 min, $h\nu$	234	258	108
C, HP	initial	144	256	160
	+60 min, $h\nu$	107	218	140
S	initial	196	226	136
	+60 min, 180 °C	173	177	127
	+60 min, $h\nu$	249	238	89

[a] C, commercial $SnBr_2$, S, synthesized $SnBr_2$. HP, pelletized at high pressure. All data are relative to Sn = 100. All samples mounted on Mo holders.

Table III. RGA Data

obsd m/e	assgnt	obsd m/e	assgnt
18.3	OH^+	113.8–119.5	Sn^+
19.4	H_2O^+	150.7–159.0	Br_2^+
78.5–81.3	Br^+, HBr^+	186.7–199.5	$SnBr^+$

X-ray photoelectron spectra for the synthesized $SnBr_2$ pellet on Mo in the Sn $3d_{3/2}$ and Sn $3d_{5/2}$ regions are shown in Figure 1. Figure 1a shows the Sn 3d transitions for the pellet before irradiation. Figure 1b shows the Sn 3d transitions for the same material of Figure 1a after photolysis.

X-ray photoelectron spectra for the Br 3d region are given in Figure 2. The relative intensities of the Br 3d transition for the commercial sample of $SnBr_2$ before photolysis are shown in Figure 2a, whereas similar data for the same material after photolysis are given in Figure 2b. There is a considerable loss in intensity of the Br 3d region after photolysis. Similar comparisons of intensity ratios of the elements O, Sn, C, and Br for all samples can be found in Table II. In all cases it is clear that there is a significant loss of Br during photolysis. Significant loss of carbon is observed in most cases during photolysis. In four out of the five entries of Table II the level of O also decreases during photolysis. All data have been normalized to the tin transitions. It appears in most of these experiments that there is significant loss of each of the observed surface elements during photolysis.

Photogravimetric Analysis. Data for photogravimetric analyses of commercial $SnBr_2$ are given in Figure 3. The initial weight of the sample is about 110.9 mg, which is shown by curve A at the upper left-hand corner of Figure 3. The lower curve (B) is the temperature of the sample during the photolysis and as a result of the irradiation. Notice that the temperature increases from about 25 to 35 °C during the photolysis as shown in Figure 3. Temperatures somewhat higher than 60 °C have been observed by direct irradiation of thermocouples inserted in this apparatus. The photolysis process has been pulsed during this experiment and was started at the points marked by an asterisk and stopped at the points marked by a prime. Note that as soon as the photolysis starts that the temperature starts to increase until the light is turned off. After irradiation there is some apparent gain in weight by the sample; however, there has been a significant consecutive reduction in the weight of the sample after each pulse sequence of irradiation.

Photogravimetric analysis data for the synthesized $SnBr_2$ sample are given in Figure 4. The symbols used in Figure 4 are the same as those used in Figure 3. In this case it

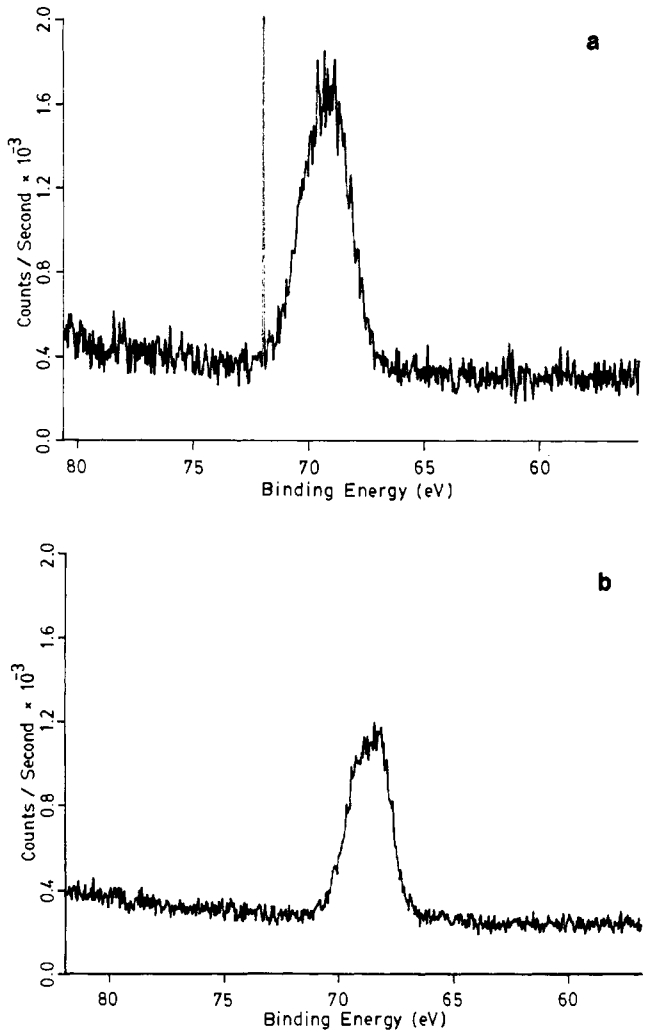

Figure 2. X-ray photoelectron spectra of the Br 3d transitions for impure $SnBr_2$ on Mo: (a) no irradiation; (b) irradiated with 1000-W Xe lamp for j0 min.

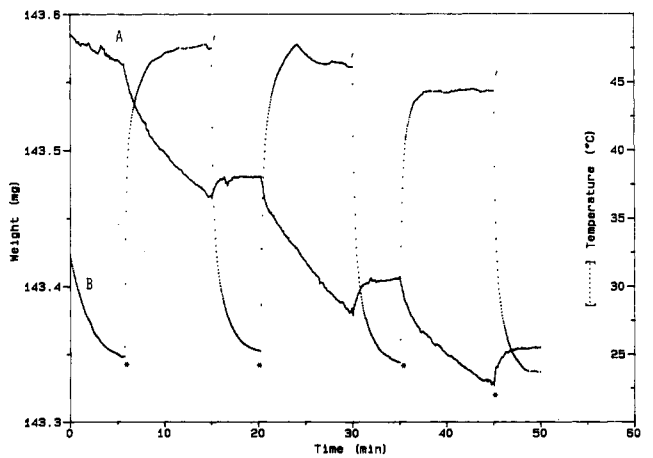

Figure 3. Photogravimetric analysis of impure $SnBr_2$.

is clear that there is a smaller weight loss during photolysis than that observed for the commercial sample shown in Figure 3. The temperature rise is roughly the same for both the commercial and synthesized $SnBr_2$ samples.

Residual Gas Analysis. Table III includes peaks observed with a residual gas analyzer during the photolysis of commercial $SnBr_2$ on Mo in the preparatory chamber of the surface instrument. Peaks at 18.3, 19.4, 78.5–81.3, 113.8–119.5, 150.7–159, and 186.7–199.5 were observed. The relative intensities of these peaks are as follows: 18.3,

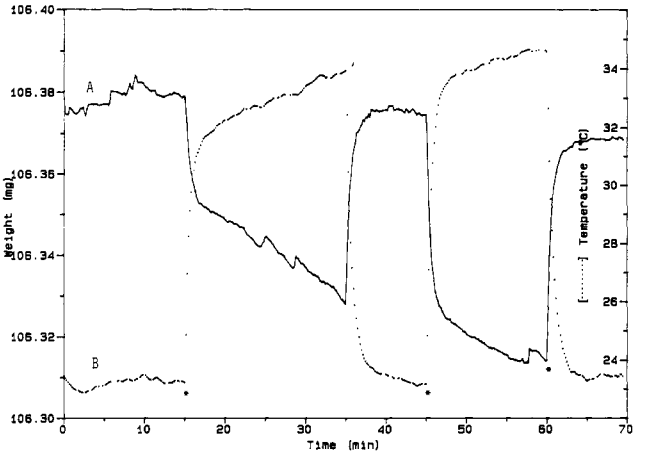

Figure 4. Photogravimetric analysis of purified $SnBr_2$.

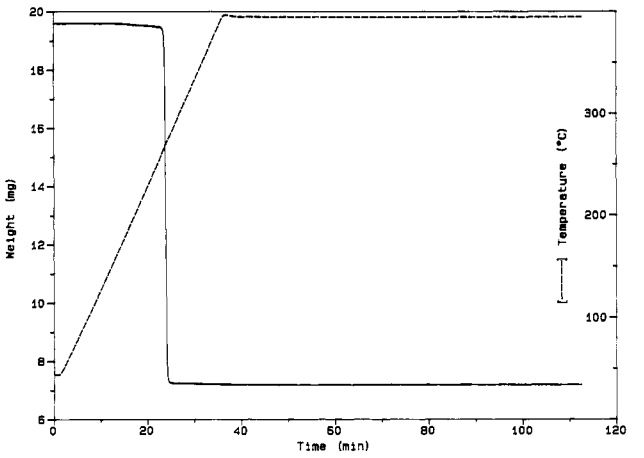

Figure 5. Thermogravimetric analysis of impure $SnBr_2$.

19.4 (100); 78.5–81.3 (50); 113.8–119.5 (6); 150.7–159 (2); 186.7–194.5 (25). Similar RGA experiments were done on other samples. For the synthesized $SnBr_2$ samples, similar m/e peak positions were observed although the relative intensity of the 18 and 19 peaks were much smaller than that of the commercial $SnBr_2$ sample.

Thermogravimetric Analysis. Thermogravimetric analyses were done on samples at temperatures up to 65 °C to simulate the temperature increase observed in the photogravimetric analyses. The observed weight changes in these TGA experiments were much lower (1%) than those of the PGA experiments. TGA experiments were done up to temperatures of 400 °C to observe weight changes and possible effects of thermal treatment. A thermogravimetric analysis for the commercial $SnBr_2$ is shown in Figure 5. At a temperature of about 275 °C there is a significant and precipitous loss in weight. To decipher differences between the commercial and synthetic $SnBr_2$ samples, the same type of TGA experiment was done on a synthetic $SnBr_2$ sample, and TGA data are given in Figure 6. Again there is a precipitous loss of weight near 275 °C. These temperatures are far above the temperatures recorded in the photogravimetric and the in situ photolytic XPS experiments.

Differential Scanning Calorimetry. Differential scanning calorimetry experiments were done on the synthetic and commercial samples of $SnBr_2$ to observe any differences between these materials. A DSC experiment of the commercial $SnBr_2$ is given in Figure 7. Major changes occur near 232.14 °C where an *endothermic* transition occurs. There are minor endothermic transitions occurring near 150 °C and between 211.31 and 221.43 °C.

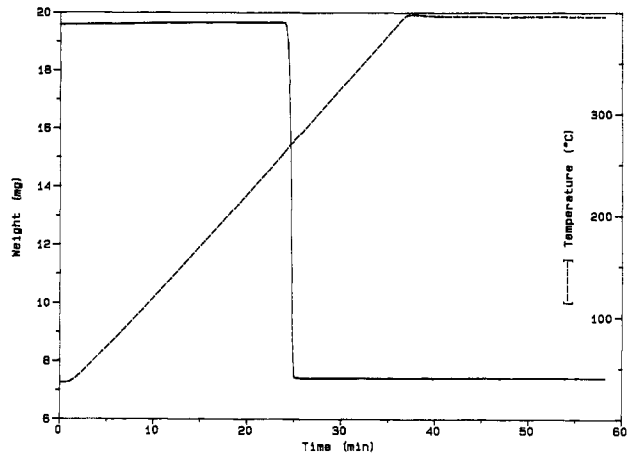

Figure 6. Thermogravimetric analysis of purified $SnBr_2$.

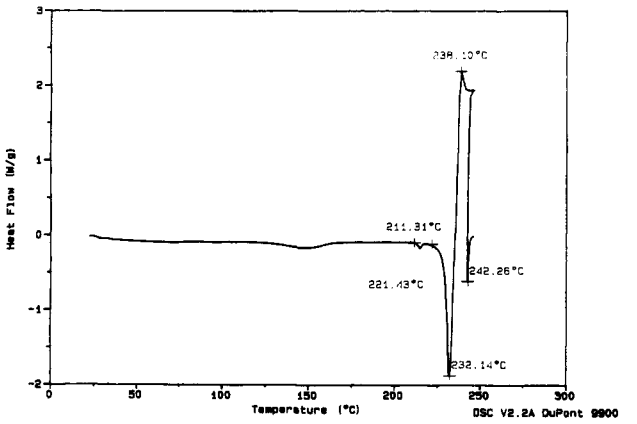

Figure 7. Differential scanning calorimetry of impure $SnBr_2$.

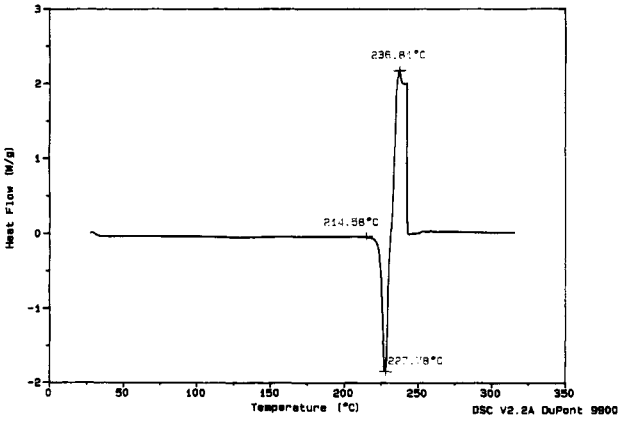

Figure 8. Differential scanning calorimetry of purified $SnBr_2$.

For comparison a DSC experiment of the synthetic $SnBr_2$ sample is given in Figure 8. There are fewer transitions for the synthetic material, although the major endotherm at 227.78 °C occurs at about the same place as the commercial sample.

Discussion. In Situ Photodegradation of $SnBr_2$. The XPS data of Table I clearly show that there is reduction of $SnBr_2$ to the metallic state. In the case of in situ photoreduction of SnS_2 it is clear that impurity chloride ions enhance the rate of reduction of the SnS_2 to metallic tin.[13]

The binding energies of the Sn, O, C, and Br transitions for the first five samples entered in Table I are remarkably

(13) Force, R. K.; Fessehaie, M. G.; Grosso, R. P.; Laliberte, J. M.; McClain, S.; Willis, W. S.; Suib, S. L. *Inorg. Chem.*, submitted.

Scheme I

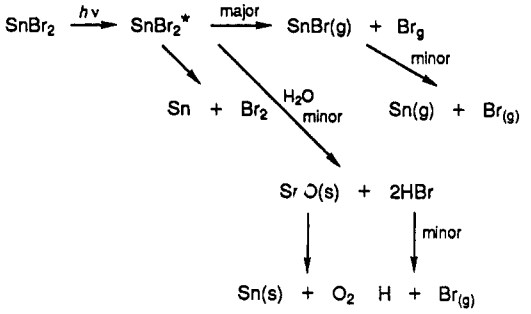

similar during thermal activation. On the other hand, photochemical activation leads to observation of Sn $3d_{3/2}$ and $3d_{5/2}$ transitions due to metallic tin. The data of Table II and Figure 2 clearly show that there are considerable changes in the amounts of the elements on the surface during photolysis. In general there is a loss of all elements after photolysis, and this is confirmed by the residual gas analyses (vide infra).

To distinguish the relative roles of surface hydroxyl and water groups on the mechanism of degradation, experiments were carried out to reduce the amounts of water and hydroxyl groups. At temperatures of 180 °C, TGA data suggest that weight loss is minimal and that most changes in weight occur in these samples at temperatures near 275 °C. We have shown that the temperatures reached during photolysis in the PGA, in situ photolytic XPS and RGA experiments do not exceed 65 °C. Even after $SnBr_2$ is heated to 180 °C, there is little change in the XPS data as shown in Table I, although the RGA data for samples heated to 180 °C show much less of a contribution from OH and H_2O.

Photogravimetric Analysis. The photogravimetric data of Figure 3 are in accord with the X-ray photoelectron spectroscopy data of Tables I and II and Figures 1 and 2. The PGA data suggest that there is considerable loss in weight during photolysis of the commercial $SnBr_2$. This weight loss is a permanent change and indicates that these samples degrade in the presence of light. Thermal activation of the same samples at the temperatures measured during these PGA experiments does not lead to reduction of the $SnBr_2$. If data[13] from photolysis of SnS_2 can be generalized to other materials, then light and impurities must be present in order to photochemically reduce these semiconductors. During photolysis there is a concomitant increase in temperature of the sample, but this increase is only about 40 °C. PGA data for the purified $SnBr_2$ sample show a small decrease in weight during photolysis.

We have shown here and elsewhere[13] that PGA methods can be used to study the photochemical stability of solids. In fact, the PGA methods are simpler and easier to perform than in situ photolytic XPS or other spectroscopic experiments. PGA methods could be used to screen the photochemical behavior of a variety of solids under vacuum or in the presence of several different gaseous atmospheres.

Mechanism of Photodegradation of Tin(II) Bromide. The RGA data of Table III show that a variety of gas-phase species are present during photolysis of $SnBr_2$. Assignments of the m/e peaks to specific gas-phase species have been made in Table III, and it appears that a considerable number of hydroxyl groups and water molecules are evolved during photolysis. The relative amounts of these gaseous species determined by RGA methods are quite helpful in determining a plausible mechanism of photodegradation of $SnBr_2$. Notice that the largest amounts of gas-phase species are OH^+, H_2O^+, Br^+, HBr^+,

and $SnBr^+$. The relative percentage of Sn^+ is very small, which is in accord with the XPS findings that little photoreduction is occurring and also suggests that $SnBr^+$ is not further fragmenting to Sn^+ and Br^+ to any appreciable extent. Taking these factors into consideration, we propose in Scheme I various major and minor pathways for the mechanisms for photodegradation of $SnBr_2$.

Several hydrates of $SnBr_2$ have been reported.[14-16] The presence of considerable amounts of water and hydroxyl groups as shown by our RGA data suggest that the surface of our $SnBr_2$ materials is hydrated. This may account for the appearance of water and hydroxyl groups during photolysis.

Conclusions

The data presented here concern the photodegradation of $SnBr_2$. Commercial $SnBr_2$ is highly contaminated with both organic and chloride impurities. Photoreduction of $SnBr_2$ to the metallic state is enhanced when significant amounts of chloride impurity ions are present on the surface. In future studies it may be possible to dope surfaces of various semiconductors with impurity ions in order to carry out the photoreduction of semiconductors. In most experiments concerning the photolysis of $SnBr_2$ we have primarily observed photofragmentation of $SnBr_2$ and to a smaller extent have observed reduction to metallic tin. The combination of XPS, RGA, PGA, and TGA experiments allows a qualitative understanding of the processes occurring on the surface of a solid during photolysis as well as information concerning evolved gaseous species. This type of information may be of importance in the design of new material to be used as catalysts, semiconductors, or as photographic materials. The photogravimetric method described here is useful for studies of the photostability of solids.

Acknowledgment. We thank the Office of Basic Energy Sciences, Division of Chemical Sciences, Department of Energy for support of this research as well as the State of Connecticut Department of Higher Education. We thank Dr. Theo Fleisch for helpful discussions.

Registry No. Br_2Sn, 10031-24-0; Sn, 7440-31-5; SnBr, 15193-66-5; Br, 10097-32-2; SnO, 21651-19-4; HBr, 10035-10-6; H_2O, 7732-18-5.

(14) Andersson, J. *Acta Chem. Scand.* **1972**, *26*, 3813.
(15) Andersson, J. *Acta Chem. Scand.* **1972**, *26*, 2543.
(16) Andersson, J. *Acta Chem. Scand.* **1972**, *26*, 1730.

Structural Transformation of Non-Oxide Chalcogenide Glasses. The Short-Range Order of Li_2S–P_2S_5 Glasses Studied by Quantitative ^{31}P and $^{6,7}Li$ High-Resolution Solid-State NMR

Hellmut Eckert,* Zhengming Zhang, and John H. Kennedy*

Department of Chemistry, University of California, Santa Barbara, Santa Barbara, California 93106

Received November 20, 1989

The local structure of crystalline and glassy compositions in the $(Li_2S)_x(P_2S_5)_{1-x}$ system is investigated by solid-state high-resolution ^{31}P, ^6Li, and ^7Li MAS NMR. Four stable crystalline pseudobinary compounds, $LiPS_3$, $Li_4P_2S_6$, Li_3PS_4, and Li_7PS_6, are identified. The ^{31}P NMR spectra obtained on amorphous samples within the region of glass formation ($0.4 \leq x \leq 0.7$) show successive formation of sulfide analogues of metaphosphate ($Q^{(2)}$), pyrophosphate ($Q^{(1)}$), and orthophosphate ($Q^{(0)}$) species with increasing concentration of lithium sulfide. The NMR studies show unusually large chemical shift changes upon the crystallization of the glasses. For $x = 0.5$ this is believed to be due to a different type of interlinking of the $Q^{(2)}$ units. For $x = 0.67$, the $P_2S_7^{4-}$ units, which are present in the glassy phase, are quantitatively destroyed upon crystallization, leading to the formation of a $P_2S_6^{4-}$ species containing a phosphorus–phosphorus bond. The NMR results illustrate the role of the glassy state in trapping metastable local environments that have no analogues in crystalline compounds.

Introduction

The discovery of very high lithium ionic conductivity in a new class of sulfide-based glasses has been one of the most significant developments in the field of solid electrolytes in the past few years.[1-13] These glasses form by rapid quenching of melts containing Li_2S, LiI, and stoichiometric group III–V sulfides, such as B_2S_3, SiS_2, and P_2S_5. Considerable experimental work has been undertaken to maximize conductivity and chemical stability of these compounds. It has been more recently that driven by the search for structural guidelines to optimize materials properties, the microstructure of these glasses has moved into the focus of attention.[14-18]

According to most recent spectroscopic studies, chalcogenide glasses can have very unusual structures, displaying

* Authors to whom correspondence should be addressed.

(1) Malugani, J. P.; Robert, G. *Solid State* Ionics **1980**, *1*, 519.
(2) Robert, G.; Malugani, J. P.; Saida, A. *Solid State Ionics* **1981**, *3/4*, 311.
(3) Malugani, J. P.; Fahys, B.; Mercier, R.; Robert, G.; Duchange, J. P.; Baudry, S.; Broussely, M.; Gabano, J. P. *Solid State Ionics* **1983**, *9/10*, 659.
(4) Mercier, E.; Malugani, J. P.; Fahys, B.; Robert, G. *Solid State Ionics* **1981**, *5*, 663.
(5) Duchange, J. P.; Malugani, J. P.; Fahys, B.; Robert, G. *Prog. Batteries Sol. Cells* **1981**, *4*, 46.
(6) Ribes, M.; Barrau, B.; Souquet, J. L. *J. Noncryst. Solids* **1980**, *38/39*, 271.
(7) Wada, H.; Menetrier, M.; Levasseur, A.; Hagenmuller, P. *Mater. Res. Bull.* **1983**, *18*, 189.
(8) Pradel, A.; Ribes, M. *Solid State Ionics* **1986**, *18/19*, 351.
(9) Kennedy, J.; Yang, Y. *J. Solid State Chem.* **1987**, *69*, 252.

0897-4756/90/2802-0273$02.50/0